A SVM Based Model for COVID Detection Using CXR Image

Sudhir Kumar Mohapatra[1], Beakal Gizachew Assefa[2(✉)], and Getamesay Belayneh[3]

[1] Faculty of Emerging Technology, Sri Sri University, Cuttack 754006, Odisha, India
sudhir.mohapatra@srisriuniversity.edu.in
[2] School of Information Technology and Engineering, AAiT, Addis Ababa, Ethiopia
beakal.gizachew@aait.edu.et
[3] School of Health, Dire Dawa University, Dire Dawa, Ethiopia

Abstract. Covid-19 is among the few global pandemic that has caused a massive adverse economic, social, and psychological effect. Nearly hundred million people are affected and out them a minimum of 2 million people lost their lives. The 2nd and 3rd wave of the spread of the virus has been recorded in the western world. Despite the countless efforts and very few successes in preparation of vaccine, the number of people who have access is very much limited even in the developed countries. The RT-PCR and antigen test are impractical in developing and underdeveloped countries because of high cost and less accuracy, respectively. Chest XRay (CXR) has been used for detection of Covid-10, however, it needs a domain expert. In this paper, we propose an Artificial Intelligent assisted automatic radiology system based on CXR images using Support Vector Machines (SVM). Experimental results conducted on real world CXR image data set shows that, our proposed system have achieved an accuracy and sensitivity of 99.4% and 86% respectively..

Keywords: CXR · Image procession · Segmentation · COVID · Support vector machine

1 Introduction

The covid-19 situation is not settled to date. In the world by 19-01-2021, 93,805,612 people were infected by the virus and 2,026,093 precious lives were lost. The figure clearly shows the alarming situation. Many European countries face the 2nd and 3rd phases of the wave. The world is still struggling to contain the virus. Though two to three vaccines are approved in the world, vaccination is restricted to a limited number of countries. The World Health Organization's advisory for the containment of the virus recommendations is testing and isolation. From different available testing methods, Reverse Transcription Polymerase Chain Reaction (RT-PCR) is considered as the golden standard [1]. Due to the challenge of building RT-PCR infrastructure and its high testing cost, developing and underdeveloped countries largely resort to an alternative low-cost testing method like testing the antigens. However, this is impractical

M. L. Berihun (Ed.): ICAST 2021, LNICST 411, pp. 368–381, 2022.
https://doi.org/10.1007/978-3-030-93709-6_24

because of the very low accuracy exhibited. The Sofia antigen test had a sensitivity of less than 37% as compared to RT-PCR tests when used for screening of asymptomatic persons [2].

The cause of COVID because of the virus SARS-CoV-2. It is a respiratory disease which affect the lungs the most. Traditionally for existing respiratory disease like tuberculosis we use Chest X-Ray (CXR) as a diagnosis method. The diagnostic center with X-Ray are adequately available in private and public health care facilities. For the identification of the disease, manual examination of CXR by a radiologist is required. The limited availability of test-kits and domain experts in the hospitals and rapid increase in the number of infected patients necessitates an automatic screening system, which can act as a second opinion for expert physicians to quickly identify the infected patients, who require immediate isolation and further clinical confirmation. It can act as an alternative screening modality for the detection of nCOVID-19 or to validate the related diagnosis, where the CXR images are interpreted by expert radiologists to look for infectious lesions associated with nCOVID-19. In this work, we proposed an AI assisted COVID-19 lung X-ray image-based detection method using SVM. The contribution of this work is as follow.

- Proposed a computer added diagnosis model for COVID-19 detection
- SVM classifier is used to avoid high computational resources and huge training and testing data set.
- Conducted experiments on a real-world data set. Experimental results show that, the proposed system exhibited an accuracy of 99.4% and sensitivity of 86%.

The remainder of the paper is organized as follows; Sect. 2 shows the related work. Sections 3 and 4 presents the proposed system and the experimental results on a real world CXR image data sets. Conclusion and future work directions are put on Sect. 5.

2 Related Works

All the world still fighting to contain and control COVID-19 pandemic. Every branch of science are contributing to it day by day. The world health organization already declare that we have to habituate to live with this virus. In this direction many research a has been done for proper diagnosis of the disease. Researcher proposed computer added diagnosis system using machine learning. The radio imaging and epidemiology findings using ML are reported by many researcher [3–6]. Going further Deep Learning models are also used for analysis of the characteristic of theses radiology images [7, 8]. with a good diceindex of 0.67, Xue et al. (2018) assign class level in CXR image for detection of a localize tuberculosis-infected regions in CXR images [9]. They use Deep Learning for this. Purkayastha, Buddi, Nuthakki, Yadav, and Gichoya (2020) successfully assigns one level out of fourteen to the uploaded CXR images [10]. Pesce et al. (2019), also able to level the images using two proposed model [11].

DL is applied by many researchers for early detection of COVID-19 [12–16]. But the main challenge face by their models are annotated images (CXR). Availability of less annotated CXR images and requirement of large data by DL increase the difficulty of the researcher. To overcome this problem different overfitting avoidance method are applied by researcher. Method like random photometric transformations like blurring,

sharpening, contrast adjustment, are implemented in their model [13, 14, 17]. The CXR images are further used to perform in-depth volumetric analysis of subtle disease responses (similar to viral pneumonia or other inflammatory lung diseases) [13, 14, 18].

After study for the available literature we find the following gaps.

- Lack of availability of enough dataset (Annotated CXR Image)
- Deep learning is data hungry which requires huge amount of data.
- Deep learning requires high computational resource which may not be easily available in developing and under developed country.

In this study, we proposed a SVM based COVID diagnosis system. The major benefit of the proposed system is low computational resource requirement and also can be trained correctly with less available annotated images.

3 Proposed Model

The application of image processing in medical diagnosis is require different processing than normal image processing. Here the CXR images are overlapped with many different organs, which make the processing difficult. The proposed model for COVID detection using CXR image will pass through many image processing steps. These steps are discuss in the following (see Fig. 1).

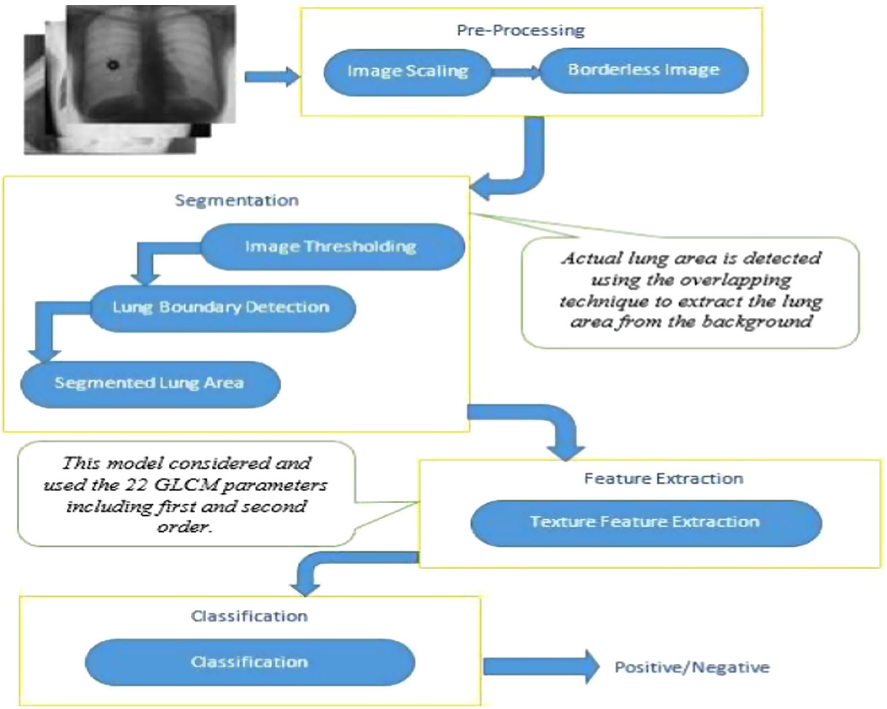

Fig. 1. The proposed model

The details of each image processing steps are discussed in the following subsections.

3.1 Preprocessing

The images in the dataset are of different resolution. For processing all the images should be made uniform by applying normalization. In the preprocessing step consist of basic and intensive task of image processing, where the model scales the image from variable resolution to uniform resolution. In this phase nonzero pixels connect to border are also removed. The model normalizes the image with 1024 × 1024 resolution because the classification is based on statistical or textural feature. The next step is to identify the lung area. To achieve it the image, need to be sharpen. The model use dilation and erosion technique of open CV. This sharpen the lung object particularly left and right side of the lungs.

3.2 Segmentation

The distortion in the CXR image para-medical professional, quality of medical equipment, poor contrast, different lung size, different shape of lung due to age of the patient are challenge for CXR image segmentation. This distorted images are display in the following (see Fig. 2).

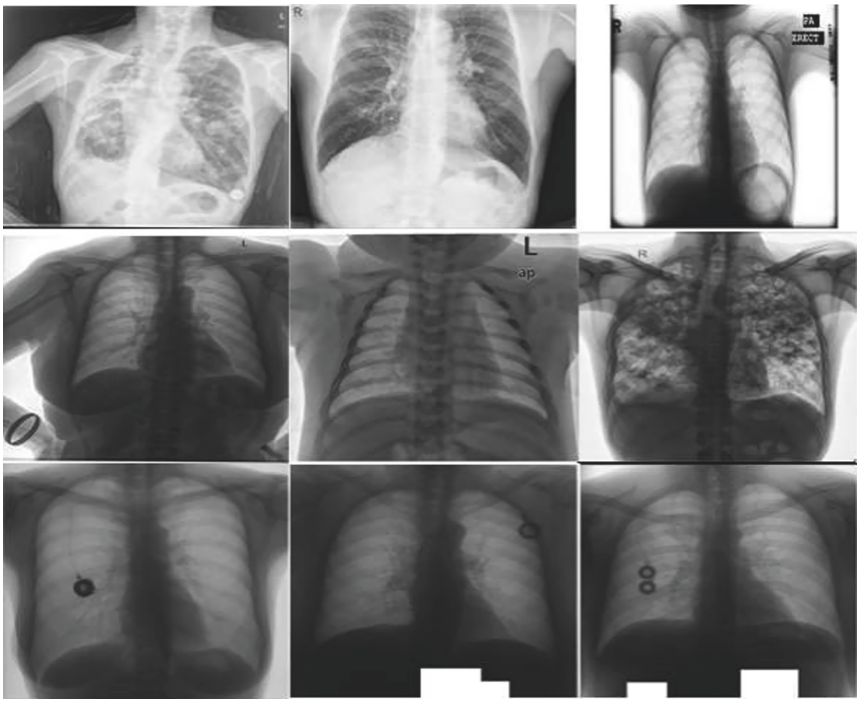

Fig. 2. Cohen JP dataset sample raw images.

The CXR image contains lung in the foreground and also some background information. The background information of the lungs need to be removed. The background information has a property i.e. these are lighter than its neighboring. To identify, remove it there are existing technique. This article applies popular clear border algorithm [19]. This algorithm is effective in cleaning of the structure. It compares the surrounding of the structure with the border of the images. The proposed model use scikit-image library of python to remove background information. Next for thresholding, Otsu thresholding [20, 21] for global and local thresholding are applied. Thresholding make it easier to extract the lungs are from the CXR image. In CXR, it is challenging to separate the lung fields using pure pixel-based approaches. Overlapping technique is used in our model for separation of lung area from the background objects (Like other organs coms in the CXR images).

3.3 Feature Extraction

Normal and abnormal images have different graylevel. In case of CXR images, the distinction of these two (Normal and Abnormal) is lie in the depth of actual color. This is because some part of the lungs are affected by SARS-CoV-2. Statistical Methods are used in our model for analysis of the appearance of a segmented region. For this the proposed model use a combination of first-order and second-order textural features extraction parameters. The effect of basic statistical methods clues to high representations of textures in an image and the gray-level histogram labels the texture of an image. The first five parameters from first order and another five from the grey level co-occurrence matrix (GLCM) features extraction parameters used in our model. These techniques shows the pixel relationship with graylevel. Grey level co-occurrence matrix was proposed was primary proposed by Haralick al. [22]. The researcher first proposed four second-order parameters such as contrast, energy, correlation and entropy. Another 22 parameters are added to it by Soh et al. [23]. Many researchers used GLCM successfully in their research ranging from image segmentation to textural feature analysis [24–26]. The texture features using GLCM are determined by seeing the rate of pixel pairs with the values which agrees the grey level in spatial connection of an image and extracting the factors from the matrix [27].

This model used other seventeen second order parameters of GLCM and they are cluster shade, difference-entropy, contrast, correlation, cluster prominence, difference-variance, dissimilarity, energy, entropy, information measure of correlation, homogeneity, maximum probability, sum average, sum entropy, sum of squares: variance and sum variance. These are used and suggested by researchers [28].

3.4 Classification

In this model, classification of lungs in terms of infected and non-infected is to achieve. The Support vector machine (SVM) classifier is better in binary classification among available classifier [29, 30]. The classification of normal and abnormal images is done by the help of hyper plane generate by SVM with a linear classifier. The scikit-learn library in python is used to apply SVM using Radial Basis Function Kernel. The performance evaluation of the model is done by separating the dataset into train and test set. The K-fold technique of cross validation is used.

4 Experiments and Results

Google Colaboratory GPU environment used for the experiment purpose. The model is implemented in Python3 with scikit-learnlibrary. The next subsection discuss about the details of individual sub-process.

4.1 Dataset Preparation

The public datasets of CXR imagesare considered for experiment [32]. The CXR images collected from Github repository of Cohen JP[1] is used for training and validation of our model. It is continuously updated by different researcher from different geographical area. This open dataset is having normal, infected and pneumonia affected images (see Fig. 3).

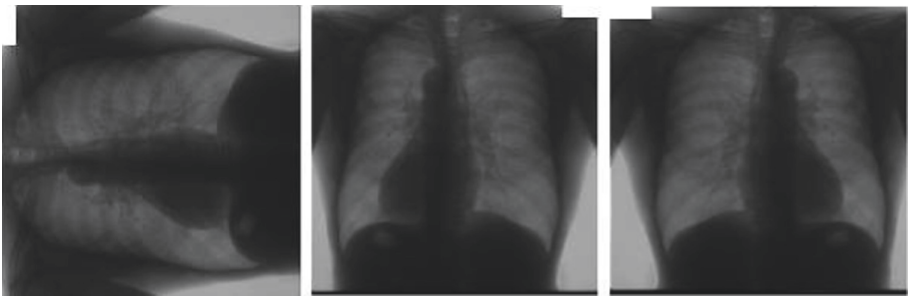

Fig. 3. Slicing image for the dataset

[1] https://github.com/muhammedtalo/COVID-19.

4.2 Preprocessing

The model requires standardized uniform images. To achieve it, CXR images from the data set are resize to 1024 × 1024 using OpenCV. The images then go through a process of removal of lighter information. This is done by first assuming lighter information as background information and looking into its connection to the border (see Fig. 4).

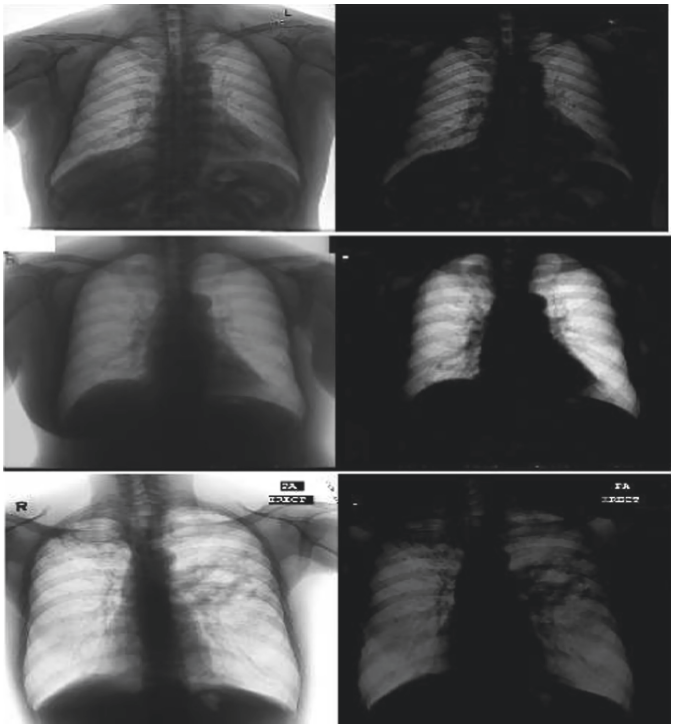

Fig. 4. The dataset images after sampling

Next using Otsu threshold algorithm and threshold value of 0.01, 0.001 the borderless image are change to binary image [20, 33]. Then, filtering method is used to the two lungs with a input value of 2. The filtering further applies hole fill method find out hole. The presence of hole in lungs indicate the presence of infection of COVID or distortion of image. All the above discussion are presented with input output images (see Fig. 5).

4.3 Detection of Lung Region

After identifying the lungs object, next issue may be unclear boundary. To achieve this python and OpenCV is used. The input and output of the process are presented in

A) Original Image	B) Border less Image	C) Binaries	D) Thresholding With 0.01	E) Thresholding With 0.001	F) Global Otsu's threshold

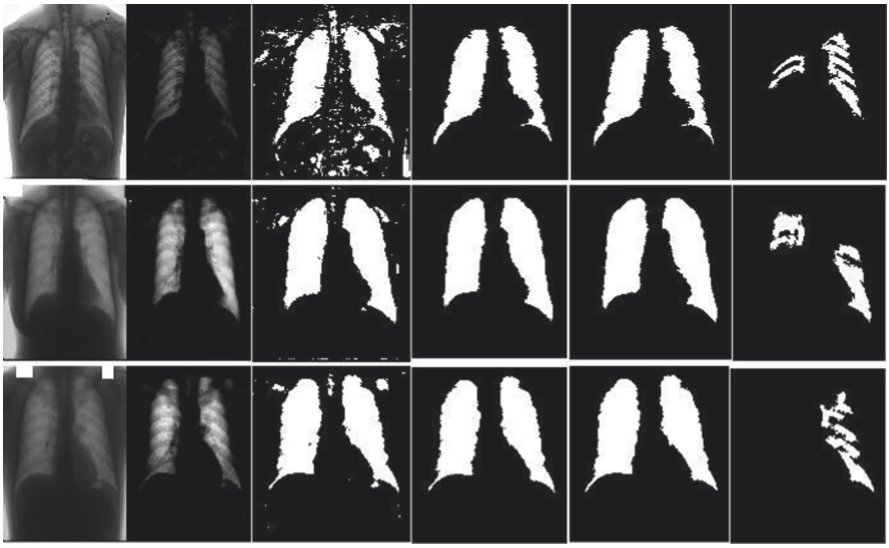

Fig. 5. Image after different filtering method

Fig. 6. The first column A contains original image, column B contains detected object and the last column(c) contains (see Fig. 6).

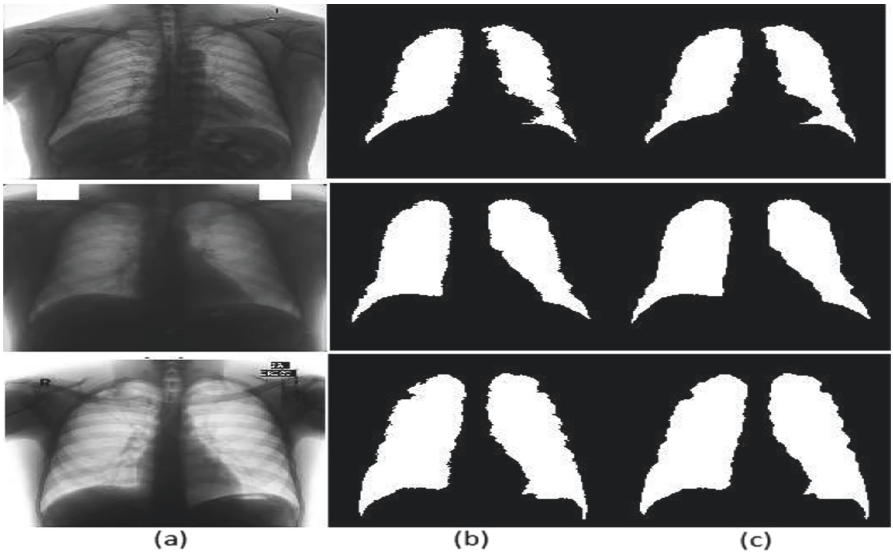

Fig. 6. Lungs area sharpening using dilation

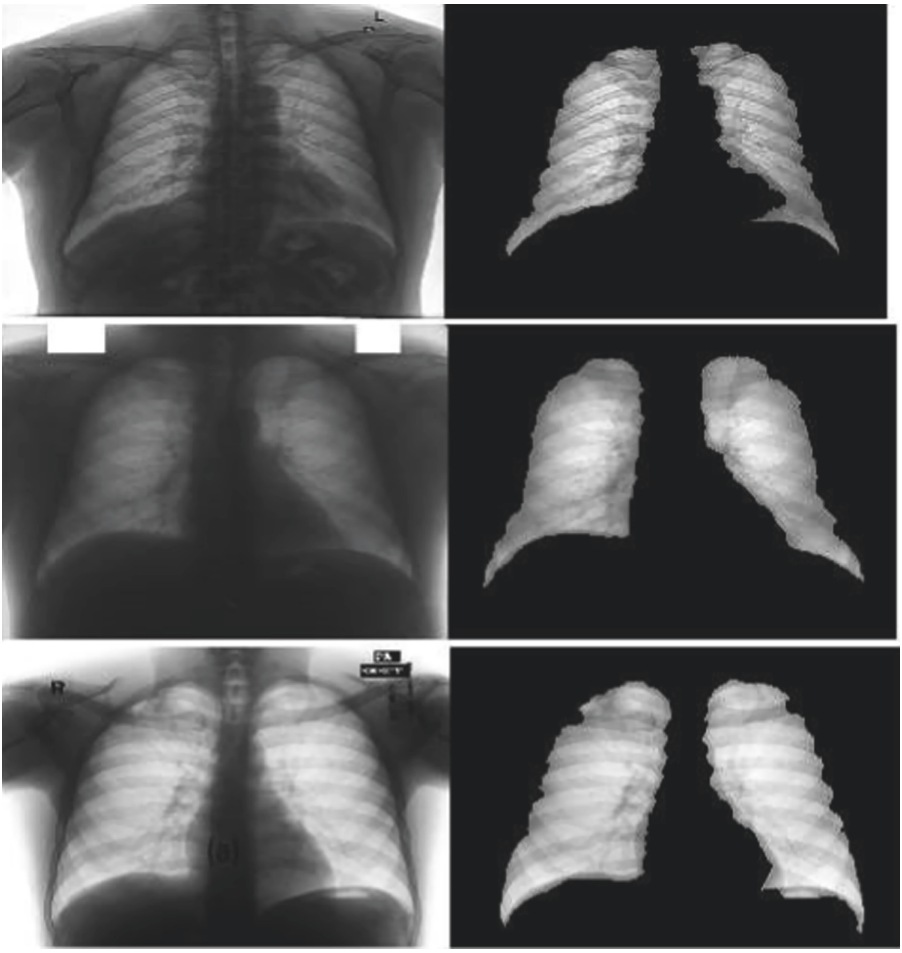

Fig. 7. Segmentation from the open data set.

4.4 Segmentation

In segmentation the lung object is extracted from the CXR images. It is a process where except the lung object all other organs are treated as background object. As the lung area in the binary image is in white in color, the model extracts the white region only. In the process the same white intensity area with actual intensity is considered. The other area intensity makes 0 or black. Figure 7 present the whole segmentation steps (see Fig. 7).

4.5 Feature Extraction

Python3 and Scikit-image is used to apply the feature extraction step.Allthe first order and second order parameter are stored in a excel file for SVM processing. Figure 8 present a sample extracted feature (see Fig. 8).

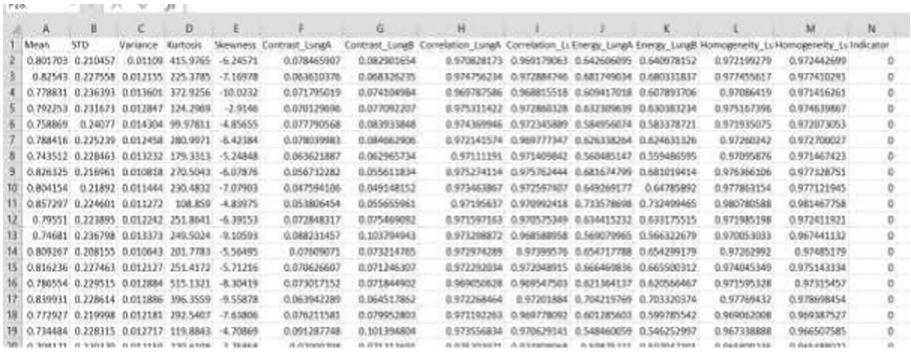

	A	B	C	D	E	F	G	H	I	J	K	L	M	N
1	Mean	STD	Variance	Kurtosis	Skewness	Contrast_LungA	Contrast_LungB	Correlation_LungA	Correlation_Lu	Energy_LungA	Energy_LungB	Homogeneity_Lu	Homogeneity_Lu	Indicator
2	0.801703	0.210457	0.01109	415.9765	-6.24571	0.078465907	0.082901654	0.970828173	0.969179063	0.642606895	0.640978152	0.972199279	0.972442699	0
3	0.82543	0.227558	0.012155	225.3785	-7.16978	0.063610376	0.068326235	0.974756234	0.972884746	0.681749034	0.680331837	0.977455617	0.977410291	0
4	0.778831	0.236393	0.013601	372.9256	-10.0232	0.071795019	0.074104984	0.969787586	0.968815518	0.609417018	0.607893706	0.97086419	0.971416261	0
5	0.792253	0.231673	0.012847	124.2909	-2.9146	0.070129696	0.077092207	0.975311422	0.972860328	0.632309639	0.630383234	0.975167396	0.974639867	0
6	0.758869	0.24077	0.014304	99.97811	-4.85655	0.077790568	0.083933848	0.974369946	0.972345889	0.584956074	0.583378721	0.971935075	0.972073053	0
7	0.788416	0.225239	0.012458	280.9971	-6.42184	0.078039983	0.084682906	0.972141574	0.969777347	0.626338264	0.624631326	0.97260242	0.972700027	0
8	0.743512	0.228463	0.013232	179.3313	-5.24848	0.063621887	0.062965734	0.97111191	0.971409842	0.560485147	0.559486595	0.97095876	0.971467423	0
9	0.826325	0.216961	0.010818	270.5043	-6.07876	0.056732282	0.055611834	0.975234114	0.975762444	0.683674799	0.681019414	0.976366106	0.977128751	0
10	0.804154	0.21892	0.011444	230.4832	-7.07903	0.047594106	0.049148152	0.973463867	0.972567407	0.649269177	0.64785892	0.977863154	0.977121945	0
11	0.857297	0.224601	0.011272	108.859	-4.83975	0.053806454	0.055655961	0.97195637	0.970992418	0.733578698	0.732490465	0.980780588	0.981467758	0
12	0.79551	0.223895	0.011242	251.8641	-6.39153	0.072848317	0.075469092	0.971597163	0.970575349	0.634415232	0.633175515	0.971985198	0.972411921	0
13	0.74681	0.236798	0.013373	249.5024	-9.10593	0.088231457	0.103794943	0.973298872	0.968588958	0.569079965	0.566322679	0.970053033	0.967441132	0
14	0.809267	0.208155	0.010643	201.7783	-5.56495	0.07609071	0.073214765	0.972974289	0.97399576	0.654717788	0.654299179	0.97262992	0.97485179	0
15	0.816236	0.227463	0.012127	251.4172	-5.71216	0.070626607	0.071246307	0.972292034	0.972048915	0.666469836	0.665500312	0.974045349	0.975143334	0
16	0.786554	0.229515	0.012884	515.1321	-8.30419	0.073017152	0.071844902	0.969050628	0.969547503	0.621364137	0.620566467	0.971595328	0.97315457	0
17	0.839931	0.228614	0.011886	396.3559	-9.55878	0.063942289	0.064517862	0.972268464	0.97201884	0.704219769	0.703320374	0.97769432	0.978698454	0
18	0.772927	0.219998	0.012181	292.5407	-7.63806	0.076211581	0.079952803	0.971192263	0.969778092	0.601285603	0.59978554	0.969062008	0.969387527	0
19	0.734484	0.228315	0.012717	119.8843	-4.70869	0.091287748	0.101394804	0.973556834	0.970629143	0.548460059	0.546252997	0.967338888	0.966507585	0

Fig. 8. Sample of extracted feature in an Excel format.

4.6 The Performance Evaluation

The datasets are separated as train and test sets. The cross-validation [31], particularly the kfolds technique was used is used in our model. This model use 10-fold method.

4.7 Result

After feature extraction the confusion matrix of the pubic dataset with train and test dataset is shown in Table 1. From the table out of total 662 instance 522 images are correctly detected, 6 are incorrectly detected. These are also crosscheck by human expertise. The following Table 1.

Table 1. Confusion matrix.

Dataset		Positive	Negative	Total
Cohen JP	Normal	324	2	662
	Abnormal	4	332	

The confusion matrix shows a performance of around 99.4 accuracy and 86% sensitivity. The performance matrix in the following Table 2.

Table 2. Performance analysis of the model

Dataset	Area under curve (AUC)	Specificity (%)	Accuracy (%)	Sensitivity (%)
Cohen JP	0.99	81	99.4	86

The overall performance of the proposed model is shown in the (see Fig. 9) by a AUC curve.

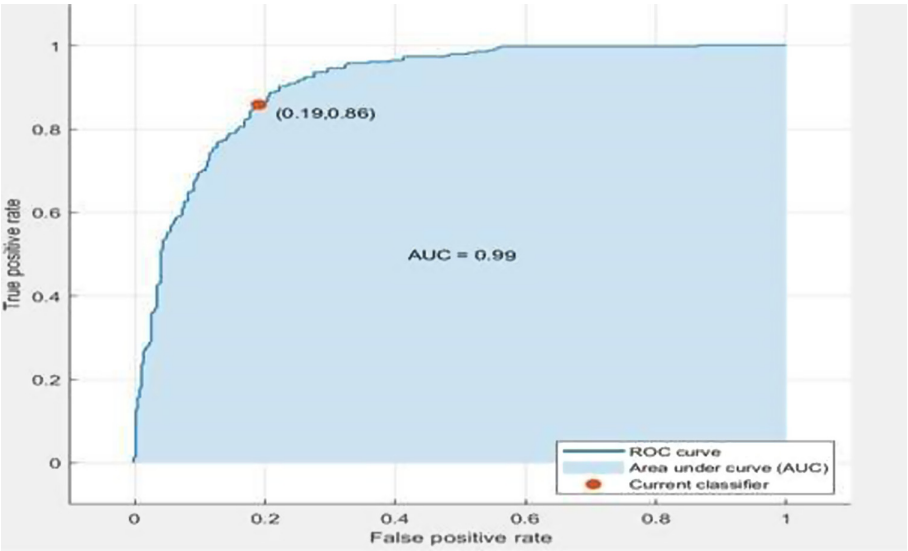

Fig. 9. ROC and AOC of the model on Cohen JP dataset

4.8 Comparison with Other Existing Models

The result achieve by the proposed model are compared with 5 deep learning model (Hemdan et al. [34], Narin et al. [35], Wang and Wong [36], Ozturk et al. [39], Nayak et al. [16]), two deep learning model combine with SVM (Sethy and Behera [37], Toğaçar et al. [38]). The comparison is presented in the Table 3. This article proposed model is classify the data set into 326 COVID 19 and 336 normal images. The proposed model use more image than all the compared technique except that of Wang et al.. But Wang et al. drawback is the technique leads to a class imbalance problem. The researcher also go for multi classification. Using binary classification and SVM our model our model performance is more than 99%. The following Table 3.

Table 3. Comparison with other models.

Authors	Used Method	Number of class	Sample Used	Accuracy (%)
Hemdan et al. [37]	COVIDX-Net	COVID-19	50	90
		Normal	C: 25 and N: 25	
Wang and Wong [39]	COVID-Net	COVID-19	13800	92.6
		Normal	C: 183	
Sethy and Behera [40]	ResNet-50 and SVM	COVID-19	50	95.38
		Normal	C: 25 and N: 25	
Narin et al. [38]	ResNet-50	COVID-19	100	98
		Normal	C: 50 and N: 50	
Ozturk et al. [42]	Dark Covid Net	COVID-19	625	98.08
		Normal	C: 125 and N: 500	
Toğaçar et al. [41]	SqueezeN et and MobileNe tV2	COVID-19	458	98.25
	SMO and SVM	Normal	C: 295, N: 65 and P: 98	
Nayak et al.[16]	ResNet-34	COVID-19	406	98.33
		Normal	C: 203 and N: 203	
Proposed Model	SVM	COVID-19	662	99.4
		Normal	C: 552 and N: 110	

5 Conclusion

The respiratory disease COVID-19 is still a global threat. This article proposed a novel SVM classifier for screening of COVID-19 patient. The study use CXR images from public dataset. The result shows accuracy of 99.4%, which is more than other Deep learning models. The model can be used in computer aided diagnosis, thereby reducing the workload of frontline health worker. It will be helpful in early identification and isolation of COVID19 patient, when all the world struggling to get vaccinated. Besides, the model requires low computational resources.

References

1. Jameel, T., Baig, M., Gazzaz, Z.J.: Persistence of reverse transcription-polymerase chain reaction (RT-PCR) positivity in COVID-19 recovered patients: a call for revised hospital discharge criteria. Cureus **12**(7), 9048 (2020). https://doi.org/10.7759/cureus.9048

2. Pray, I.W.: Performance of an antigen-based test for asymptomatic and symptomatic SARSCoV-2 testing at two university campuses—Wisconsin, September–October 2020. MMWR Morbid. Mortal. Wkly. Rep. **69** (2021)
3. Chen, N., et al.: Epidemiological and clinical characteristics of 99 cases of 2019 novel coronavirus pneumonia in Wuhan, China: a descriptive study. Lancet **395**(10223), 507–513 (2020). https://doi.org/10.1016/S0140-6736(20)30211-7
4. Huang, C., et al.: Clinical features of patients infected with 2019 novel coronavirus in Wuhan, China. Lancet **395**(10223), 497–506 (2020). https://doi.org/10.1016/S0140-6736(20)30183-5
5. Kooraki, S., Hosseiny, M., Myers, L., Gholamrezanezhad, A.: Coronavirus (COVID-19) outbreak: what the department of radiology should know. J. Am. Coll. Radiol. **17**(4), 447–451 (2020). https://doi.org/10.1016/j.jacr.2020.02.008
6. Yoon, S.H., et al.: Chest radiographic and CT findings of the 2019 Novel Coronavirus Disease (COVID19): analysis of nine patients treated in Korea. Korean J. Radiol. **21**(4), 494 (2020). https://doi.org/10.3348/kjr.2020.0132
7. Chouhan, V., et al.: A novel transfer learning based approach for pneumonia detection in chest X-ray images. Appl. Sci. **10**(2), 559 (2020). https://doi.org/10.3390/app10020559
8. Jaiswal, A.K., Tiwari, P., Kumar, S., Gupta, D., Khanna, A., Rodrigues, J.J.P.C..: Identifying pneumonia in chest X-rays: a deep learning approach. Measurement **145**, 511–518 (2019). https://doi.org/10.1016/j.measurement.2019.05.076
9. Xue, Z., et al.: Localizing tuberculosis in chest radiographs with deep learning. In: Zhang, J., Chen, P.-H. (Eds.), Medical Imaging 2018: Imaging Informatics for Healthcare, Research, and Applications, vol. 3, p. 28 (2018). https://doi.org/10.1117/12.2293022
10. Purkayastha, S., Buddi, S.B., Nuthakki, S., Yadav, B., Gichoya, J.W.: Evaluating the implementation of deep learning in LibreHealth radiology on chest X-rays. Adv. Intell. Syst. Comput. **943**, 648–657 (2020). https://doi.org/10.1007/978-3-030-17795-9_47
11. Pesce, E., Joseph Withey, S., Ypsilantis, P.P., Bakewell, R., Goh, V., Montana, G.: Learning to detect chest radiographs containing pulmonary lesions using visual attention networks. Med. Image Anal. **53**, 26–38 (2019). https://doi.org/10.1016/j.media.2018.12.007
12. Abbas, A., Abdelsamea, M.M., Gaber, M.M.: Classification of COVID-19 in chest X-ray images using DeTraC deep convolutional neural network (2020). Retrieved: http://arxiv.org/abs/2003.13815
13. Wang, S., et al.: A deep learning algorithm using CT images to screen for corona virus disease (COVID-19). MedRxiv (2020). https://doi.org/10.1101/2020.02.14.20023028
14. Xu, X., et al.: Deep learning system to screen coronavirus disease 2019 pneumonia. Arxiv (2020). Retrieved: https://arxiv.org/abs/2002.09334
15. Mishra, A.K., Das, S.K., Roy, P., Bandyopadhyay, S.: Identifying COVID19 from chest CT images: a deep convolutional neural networks based approach. J. Healthc. Eng. **2020**, 1–7 (2020). https://doi.org/10.1155/2020/8843664
16. Nayak, S.R., Nayak, D.R., Sinha, U., Arora, V., Pachori, R.B.: Application of deep learning techniques for detection of COVID-19 cases using chest X-ray images: a comprehensive study. Biomed. Signal Process. Control **64**, 102–365 (2020)
17. Chowdhury, M.E.H., et al.: Can AI help in screening Viral and COVID-19 pneumonia? (2020). Retrieved|: http://arxiv.org/abs/2003.13145
18. Maghdid, H.S., Asaad, A.T., Ghafoor, K.Z., Sadiq, A.S., Khan, M.K.: Diagnosing COVID-19 pneumonia from X-Ray and CT images using deep learning and transfer learning algorithms. Arxiv.Org. (2020). Retrieved: https://arxiv.org/abs/2004.00038
19. Soille, P.: Morphological Image Analysis: Principles and Applications. Springer Science & Business Media (2013)

20. Otsu, N.: A threshold selection method from gray-level histograms. IEEE Trans. Syst. Man Cybern. **9**(1), 62–66 (1979). https://doi.org/10.1109/TSMC.1979.4310076
21. Bradley, D., Roth, G.: Adaptive thresholding using the integral image. J. Graph. Tools **12**(2), 13–21 (2007). https://doi.org/10.1080/2151237X.2007.10129236
22. Haralick, R.M., Shanmugam, K., Dinstein, I.: Textural features for image classification. IEEE Trans. Syst. Man Cybern. **SMC-3**(6), 610–621 (1973). https://doi.org/10.1109/TSMC.1973.4309314
23. Soh, L.-K., Tsatsoulis, C.: Texture analysis of SAR sea ice imagery using gray level co-occurrence matrices. IEEE Trans. Geosci. Remote Sens. **37**(2), 780–795 (1999). https://doi.org/10.1109/36.752194
24. Tuceryan, M., Jain, A.K.: The Handbook of Pattern Recognition and Computer Vision, Chapter 2.1, Texture Analysis. World Scientific Co., pp. 207–248 (1998)
25. Hiremath, P.S., Pujari, J.: Content based image retrieval based on color, texture and shape features using image and its complement. Int. J. Comput. Sci. Secur. **1**, 25–35 (2007)
26. Palanivel, M., Duraisamy, M.: Adaptive color texture image segmentation using α-cut implemented interval type-2 fuzzy C-means. Res. J. Appl. Sci. **7**, 258–265 (2012)
27. Tsaneva, M.: Texture features for segmentation of satellite images. Cybern. Inf. Technol. **8**, 73–85 (2008)
28. Karargyris, A., et al.: Combination of texture and shape features to detect pulmonary abnormalities in digital chest X-rays. Int. J. Comput. Assist. Radiol. Surg. **11**(1), 99–106 (2016). https://doi.org/10.1007/s11548-015-1242-x
29. Kotsiantis, S.B., Zaharakis, I.D., Pintelas, P.E.: Machine learning: a review of classification and combining techniques. Artif. Intell. Rev. **26**, 159–190 (2006)
30. Hearst, M.A., Dumais, S.T., Osuna, E., Platt, J., Scholkopf, B.: Support vector machines. IEEE Intell. Syst. Appl. **13**, 18–28 (1998)
31. Golub, G.H., Heath, M., Wahba, G.: Generalized cross-validation as a method for choosing a good ridge parameter. Technometrics **21**, 215–223 (1979)
32. Jaeger, S., Candemir, S., Antani, S., Wang, Y.-X.J., Lu, P.-X., Thoma, G.: Two public chest X-ray datasets for computer-aided screening of pulmonary diseases. Quant. Imaging Med. Surg. **4**, 475–477 (2014)
33. Cheremkhin, P.A., Kurbatova, E.A.: Comparative appraisal of global and local thresholding methods for binarisation of off-axis digital holograms. Opt. Lasers Eng. **115**, 119–130 (2019)
34. Hemdan, E.E.-D., Shouman, M.A., Karar, M.E.: COVIDX-Net: a framework of deep learning classifiers to diagnose covid-19 in X-ray images, arXiv preprint arXiv:2003.11055 (2020)
35. Narin, A., Kaya, C., Pamuk, Z.: Automatic detection of coronavirus disease (COVID19) using X-ray images and deep convolutional neural networks, arXiv preprint arXiv:2003.10849 (2020)
36. Wang, L., Wong, A.: COVID-Net: a tailored deep convolutional neural network design for detection of COVID-19 cases from chest X-ray images, arXiv preprint arXiv:2003.09871 (2020)
37. Sethy, P.K., Behera, S.K.: Detection of coronavirus disease (COVID-19) based on deep features (2020). https://doi.org/10.20944/preprints202003.0300.v1
38. Toğaçar, M., Ergen, B., Cömert, Z.: COVID-19 detection using deep learning models to exploit social mimic optimization and structured chest X-ray images using fuzzy color and stacking approaches. Comput. Biol. Med. **121**, 103805 (2020)
39. Ozturk, T., Talo, M., Yildirim, E.A., Baloglu, U.B., Ozal Yildirim, U., Acharya, R.: Automated detection of COVID-19 cases using deep neural networks with X-ray images. Comput. Biol. Med. **121**, 103792 (2020). https://doi.org/10.1016/j.compbiomed.2020.103792